Journal of Engineering Science and Technology
Vol. 3, No. 1 (2008) 62 - 70

NUCLEATION STUDIES OF GOLD ON CARBON ELECTRODES

S. SOBRI[1]*, S. ROY[2]

[1]Department of Chemical and Environmental Engineering, Faculty of Engineering, Universiti Putra Malaysia, 43400 Serdang, Selangor, MALAYSIA
[2]School of Chemical Engineering and Advanced Materials, Merz Court, University of Newcastle upon Tyne, NE1 7RU, UK
*Corresponding Author: eeza@eng.upm.edu.my

Abstract

Interest has grown in developing non-toxic electrolytes for gold electrodeposition to replace the conventional cyanide-based bath for long term sustainability of gold electroplating. A solution containing thiosulphate and sulphite has been developed specially for microelectronics applications. However, at the end of the electrodeposition process, the spent electrolyte can contain a significant amount of gold in solution. This study has been initiated to investigate the feasibility of gold recovery from a spent thiosulphate-sulphite electrolyte. We have used flat-plate glassy carbon and graphite electrodes to study the mechanism of nucleation and crystal growth of gold deposition from the spent electrolyte. It was found that at the early stages of reduction process, the deposition of gold on glassy carbon exhibits an instantaneous nucleation of non-overlapping particles. At longer times, the particles begin to overlap and the deposition follows a classic progressive nucleation phenomenon. On the other hand, deposition of gold on graphite does not follow the classical nucleation phenomena.

Keywords: Gold nucleation, Thiosulphate-sulphite, Glassy carbon, Graphite.

1. Introduction

The emerging use of gold-based connectors in microtechnology has initiated the need to search for stable and non-toxic electrolytes for gold electrodeposition because the classical cyanide-based bath has been found to be incompatible with

Nomenclatures

A	Amps
c	Concentration, $molm^{-3}$
D	Diffusion coefficient m^2s^{-1}
F	Faraday constant, $Cmol^{-1}$
I	Current, A
I_m	Current maximum, A
j	Current density, Acm^{-2}
M	Molas mass, $gmol^{-1}$
n	Number of electrons exchanged in an electrochemical reaction, dimensionless
N_o	Number of active sites on electrode surface where nucleation can occur, cm^{-2}
t	Time, s
t_m	Time maximum, s
V	Volts
α	Charge transfer coefficient, dimensionless
π	Pi, dimensionless
P	Density, kgm^{-3}

positive photoresists used during the process [1-5]. One electrolyte that is being examined is a solution containing thiosulphate and sulphite, which was initially proposed by Osaka and co-workers [1]. This electrolyte was reported to be highly stable, requires no stabilizing additives and contained phosphoric acid as buffering agent.

Recently, a mixed thiosulphate-sulphite ligand bath has been formulated by Newcastle University with aurochloric acid, Au (III) Cl^{-4} as the starting material [2]. Subsequent reduction and complexation by thiosulphate led to formation of $Au(S_2O_3)_2^{3-}$. This electrolyte was found to be stable at near neutral pH and showed good compatibility with positive photoresists [3]. The mixed ligand bath is proved to be satisfactory for an industrial process and used as electrolyte to electrodeposit gold for microelectronics applications.

Since the discharge of gold with effluent is a major economic as well as environmental concern, this study is aimed to investigate if gold can be recovered from aged thiosulphate-sulphite electrolyte and to determine the microstructure of the obtained deposits/particles. Currently, there is no reliable information concerning gold recovery from thiosulphate-sulphite plating baths. The recovery process is expected to have an enhanced value if the recovered gold can be tailored for suitable applications, for example, gold nanoparticles are useful in catalysis, sensors, electronics etc [6-8].

2. Materials and Methods

Glassy carbon (Goodfellow Cambridge Ltd, UK) has been used as an electrode. The substrate was 99.5% pure with 1 mm thickness. The electrode was cut into 1

cm^2 and attached to a copper wire using silver loaded epoxy adhesive and hardener (RS Components, UK). In order to avoid metal deposition on copper wire and silver paste used for contact, the metallic area was covered using multi-purpose silicone sealant (Dow Corning Ltd, UK).

Gold was deposited from the thiosulphate-sulphite aged electrolyte. The bath mainly consist of $Au(S_2O_3)_2^{3-}$ as well as trace amounts of Na^+ ions. The concentration of the predominant species, Au+, was 8.981 gms/L. The electrochemical experiments were performed in a three-electrode H-cell. The cell was separated into the anode and cathode compartment by a glass frit. 45 ± 1 ml volume of aged gold thiosulphate-sulphite plating solution was equally divided in each compartment.

A potentiostat (Sycopel Scientific) controlled by a computer was used to carry out the experiments. The working electrode was mounted in the cell and held in place by the use of a metal clip. 2.0 x 2.5 cm^2 platinised-titanium sheet was used as the auxiliary electrode. All potential measurements were made with respect to a saturated mercurous sulphate electrode (SMSE).

Current-time transients were accomplished by applying the potentials from the rest potential to the deposition potentials of lower than – 0.7 V for duration of 60 seconds. Prior to each chronoamperometry measurements, the carbon surface was gently polished using wet silicon carbide paper grit 4000 (Struers Ltd., UK) and then washed thoroughly with distilled water before being transferred to the experimental cell.

In order to study the growth of gold with time, a set of current-time transients were accomplished by applying the potentials from the rest potential to the deposition potentials of – 0.925 V and - 1.20 V, for duration of 1, 10, 100, 500 and 1000 seconds. Atomic Force Microscopy (AFM) analysis for gold deposits was recorded using a Nanoscope Dimension^{TM} 3100 with operational frequency of 2 Hz. The AFM was operated in contact mode, scanning at 25 μm imaging resolutions. Scanning Electron Microscopy (SEM) analysis was also performed using a Hitachi model SE570 SEM at an acceleration voltage of 20 kV.

3. Results and Discussion

3.1 Current-time transients

Current-time transients for studying the nucleation and growth of gold was accomplished by applying the potentials from the rest potential to the deposition potentials of lower than – 0.7 V for duration of 60 seconds. In the case of gold nucleation on glassy carbon electrode, three regions of interest were typically identified in the current transients, as is shown in Fig. 1.

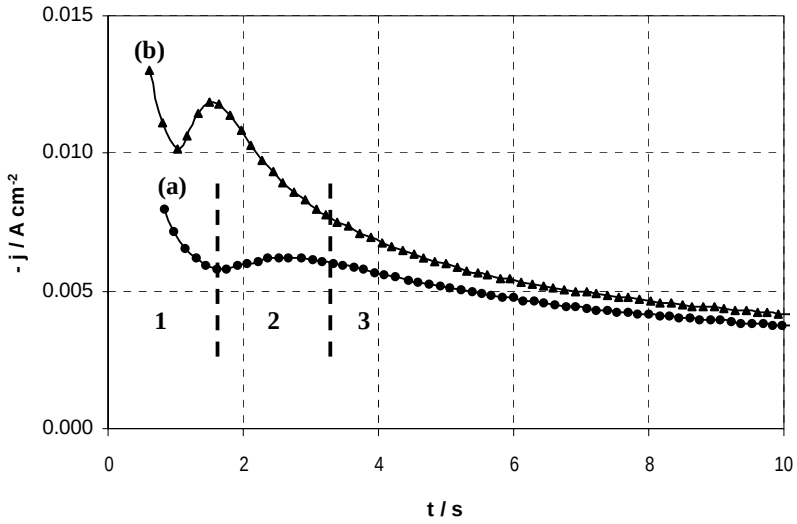

Fig. 1. Current-Time Transient for Nucleation of Gold on Glassy Carbon at (a) – 0.850 V and (b) – 0.925 V

For the first two seconds after application of a potential, there is a sharp decay in the current, mainly due to capacitive charging [9, 10] and decay of local currents [9]. The capacitive current increased with applied potential, but the time required for the decay decreased. In our analysis, current data for the first two seconds were, therefore, not used.

After the initial decay, the current transient exhibited a hump or a shoulder (for potentials greater than - 0.850 V). As the applied potential is lowered, this current maximum became more pronounced and its height and position increased as the applied potential became more cathodic, as predicted by classic nucleation phenomena [11-13]. At longer time intervals, the current reached a plateau of - 0.003 A cm^{-2}.

The potentiostatic current transient of gold on graphite, an example of which is presented in figure 2 also exhibited an initial current decay. However, unlike gold deposition on glassy carbon, no current maximum was observed in the transient, showing that classic nucleation phenomenon is not followed. The long-term current transient data approached a current density of - 0.005 A cm^{-2}, which is somewhat higher than that of glassy carbon. This could be due to a higher surface area of graphite.

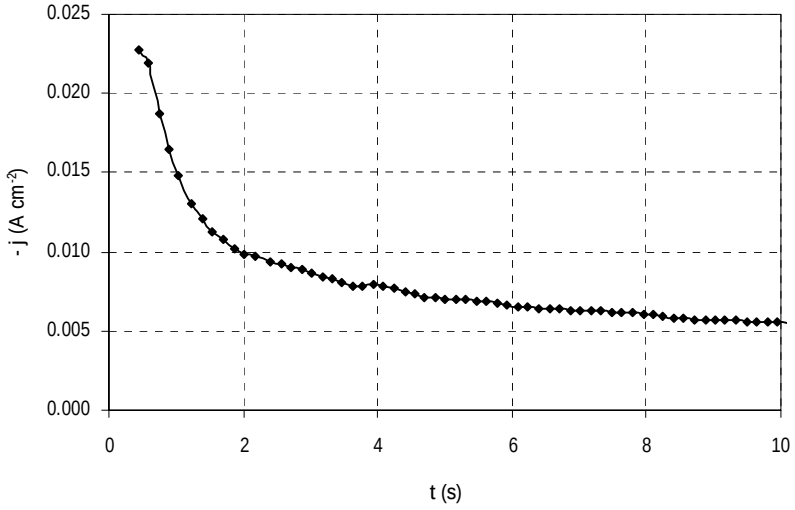

Fig. 2. Current-Time Transient for Nucleation of Gold on Graphite at – 1.05 V

3.2 Nucleation phenomena

The nucleation characteristics of gold on glassy carbon were analyzed using data from the rising part as well as the current maximum observed in region 2 of the current time transient. At the early stage of electrochemical nucleation on glassy carbon, the nuclei are widely spaced, thus it was assumed that there was no interaction between nuclei during this time. The experimental j *vs*. t data, therefore, can be described by equation 1 for the regime well before the maximum in the observed current transient.

$$I(t) = \alpha t^{v} \tag{1}$$

For the case of instantaneous nucleation, v is ½ and α is described by equations 2 and 3 for hemispherical nuclei growing under planar and spherical diffusion, respectively.

$$\alpha = \frac{8nFM^2c^3D^{3/2}}{\rho^2\pi^{1/2}}N_o \tag{2}$$

$$\alpha = \frac{nF\pi M^{1/2}(2Dc)^{3/2}}{\rho^{1/2}}N_o \tag{3}$$

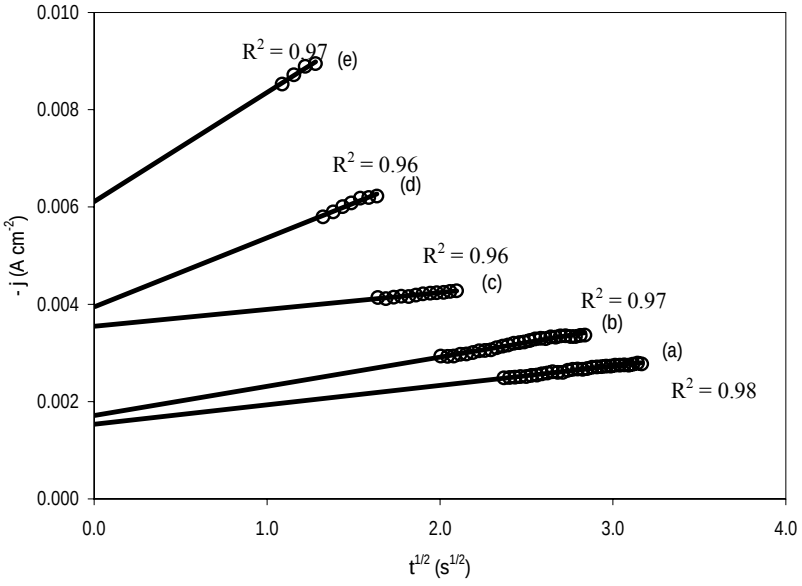

Fig. 3. Linear Dependence between j and $t^{1/2}$ Corresponds to the Early Stage of Gold Deposition on Glassy Carbon at Overpotentials (a) – 0.775 V (b) – 0.800 V (c) – 0.825 V (d) – 0.850 V and (e) – 0.875 V.

The result in figure 3 shows that a plot of j *vs*. $t^{1/2}$ observes linearity in region well before the current maximum in the current transient, indicative of hemispherical growth under instantaneous nucleation.

As the radii of nuclei increase, diffusion zones begin to overlap [10, 14]. This part of the current transient is represent by the current maximum, which is located between regions 2 and 3. This portion of the current transient is interpreted by plotting a dimensionless (or reduced) current transient, I^2/I_m^2 *vs.* the dimensionless inverse time, $(t/t_m)^{-1}$. Such a plot for glassy carbon at overpotential of - 0.85 V is shown in figure 4. It should be noted that since the dimensionless current is plotted as a function of dimensionless inverse time, the short time data of figure 1 translates to the larger values of $\left(t/t_m\right)^{-1}$ in Fig. 4.

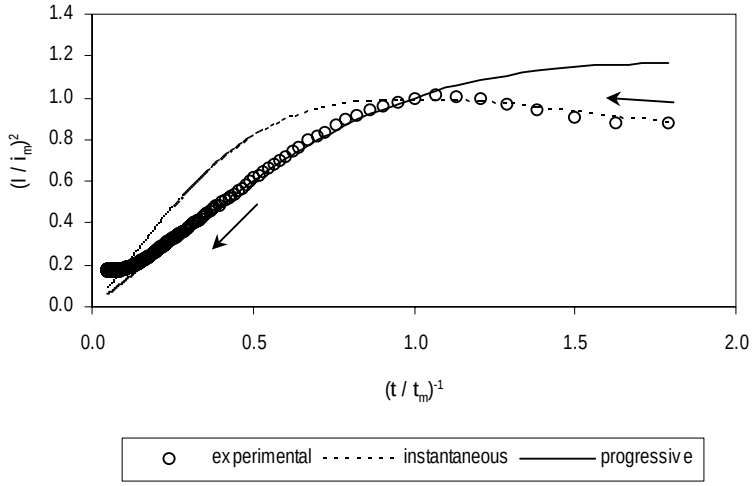

Fig. 4. Dimensionless Current-Time Transient for Nucleation of Gold on Glassy Carbon at – 0.850 V and Corresponding Theoretical Curves for Instantaneous and Progressive Nucleation.

As shown in Fig. 4, the reduced data for short time current transient is well represented by equation 2, which described instantaneous nucleation under planar diffusion. However, the data representing current maximum of the dimensionless current transient, is best represented by equation 4 below, which describes progressive nucleation.

$$\frac{I^2}{I_m^2}=\frac{1.2254}{t/t_m}\left\{1-exp\left[-2.3367\left(t/t_m\right)^2\right]\right\}^2 \quad (4)$$

These analyses indicate that the early stages of nucleation of gold is characterised by instantaneous nucleation, which changes to progressive nucleation as time proceeds. Different behaviour was observed for gold reduction from other electrolytes. In the case of gold nucleation from plating baths containing Au (III) in chloride [15, 16] and citrate [9], the electrocrystallisation mechanism changes from progressive nucleation at the early stages to three-dimensional instantaneous nucleation at longer times.

As shown in the potentiostatic current transient of gold on graphite, Fig. 2, no current maximum was observed in the transient therefore no classic nucleation analyses could be carried out. This characteristic was affirmed by the observed microscopy images of graphite, shown in the next section.

3.3 Deposit characterisation

Figure 5 shows the distribution of Au nuclei at an overpotential of -1.2 V for short (1 s), intermediate (10 s) and long (100 s) deposition times. Although the images obtained at short time were during the current decay, it can be seen that nuclei are deposited during the period of capacitive charging. The images presented indicate that the electrodeposition of Au on glassy carbon for 1 s results in uniform coverage of Au nuclei having a relatively uniform size of 80 ± 5 nm. It is also

observed that each nuclei grows independently during this stage. At the intermediate period, there is some coalescence of Au crystals and at longer times, large aggregates having diameter ranging from 100 to 300 nm are obtained.

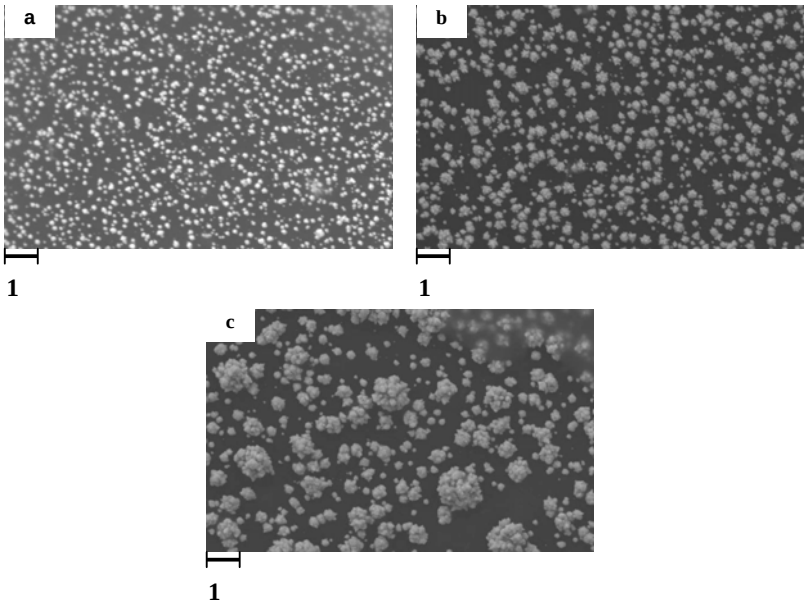

Fig. 5. SEM Images of Gold on Glassy Carbon as a Function of Deposition Time: (a) 1 s, (b) 10 s and (c) 100 s.

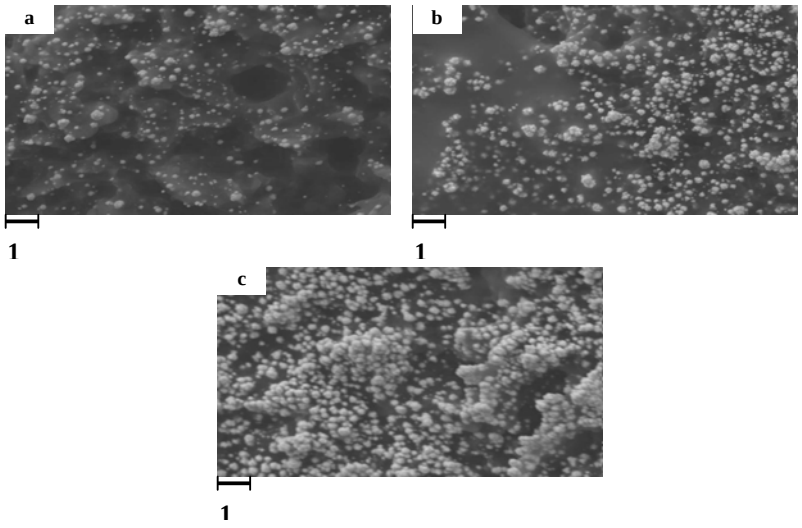

Fig. 6. SEM Images of Gold on Graphite as a Function of Deposition Time: (a) 1 s (b) 10 s and (c) 100 s.

On the other hand, Fig. 6 shows that the graphite electrode itself is rough and is characterized by craters. Gold was distributed unevenly on the surface, which is

indicative that some part of the electrode behaved as a non-planar surface. This observation confirmed that the nucleation of gold on graphite does not follow the classical nucleation phenomena.

Figure 6 also shows that numerous nuclei are formed on the planar areas, and it is clear that coalescence of the nuclei occurs even before the first second has elapsed. Between 1 and 10 s, a fraction of the Au nanoparticles continues to grow to over 90 nm while other nuclei remain in the range between 80-90 nm. After 100 s, the graphite surface is almost completely covered by Au nuclei of 100-300 nm, which have clearly coalesced from smaller nuclei. The appearance of gold deposited on graphite is more powdery than that observed for glassy carbon.

4. Conclusions

We have used glassy carbon and graphite as electrodes to study the nucleation mechanism of gold on carbon electrodes. The two different forms of carbon were chosen due to the differences in their structures. It was found that at the early stages of reduction process, the deposition of gold on glassy carbon exhibits an instantaneous nucleation of non-overlapping particles. At longer times, the particles begin to overlap and the deposition follows a classic progressive nucleation phenomenon. Deposition of gold on graphite, however, does not follow the classical nucleation phenomenon.

References

1. T. Osaka, M. Kato, J. Sato, K. Yoshizawa, T. Homma, Y. Okinaka and O. Yushioka (2001). *J. Electrochem. Soc.*, 148, C659.
2. M. J. Liew , S. Roy and K. Scott (2003). *Green Chem.*, 5, 376.
3. T. A Green, M. J. Liew and S. Roy (2003). *J. Electrochem. Soc.*, 150, C104.
4. M. J. Liew (July 2002). PhD Thesis, University of Newcastle upon Tyne, UK.
5. H. Watanabe, S. Hayashi and H. Honma (1999). *J. Electrochem. Soc.*, 146, 574.
6. G. J. Hutchings (1996). Gold Bull. (Geneva), 29 (4), 123.
7. C. W. Corti, R. J. Holliday and D. T. Thompson (2002). Gold Bull. (Geneva), 35 (4), 111.
8. P. Goodman (2002). Gold Bull. (Geneva), 35 (1), 21.
9. Y. G. Li, W. Chrzanowski and A. Lasia (1996)l. Electrochem., 26, 843.
10. B. Scharifker, *Electrochim* (1983) 28 (7), 879.
11. G. Gunawardena, Graham Hills, Irene Montenegro and Benjamin Scharifker. (1982). *J. Electroanal. Chem.*, 138, 225.
12. B. R. Scharifker and J. Mostany. (1984). *J. Electroanal. Chem.*, 177, 13.
13. P. Allongue and E. Souteyrand. (1990). *J. Electroanal. Chem.*, 286, 217.
14. G.A. Gunawardena, G. J. Hills and Irene Montenegro. (1978). Electrochim. Acta, 23, 693.
15. U. Schmidt, M. Donten and J. G. Osteryoung. (1977). *J. Electrochem. Soc.*, 144 (6) 2013.
16. Michael O. Finot, G. D. Braybrook, M. T. McDermott. (1999). *J. Electroanal. Chem*., 466, 234.